Supporting information

Phase transition in V-doped cobalt hydroxide for superior alkaline hydrogen evolution reaction†

Mengmeng Shao,*[a] Haodeng Chen,[a] Yongyong Cao,*[b] Shushu Fu,[c] Shiji Hao,[a] Min Chen,[a] Jutao Jin,[a] Wenlong, Wang,[a] Yunhui Wu[a] and Lifeng Cui*[d]

a School of Materials Science and Engineering, Dongguan University of Technology, Dongguan 523808, China.
E-mail: shaomm@dgut.edu.cn
b College of Biological, Chemical Science and Engineering, Jiaxing University, Jiaxing 314001, China.
E-mail: cyy@zjxu.edu.cn
c School of Environment and Civil Engineering, Dongguan University of Technology, Dongguan 523808, China.
d College of Smart Energy, Shanghai Jiao Tong University, Shanghai 200240, China.
E-mail: cui_lifeng@sjtu.edu.cn

This file includes Fig. S1-S11, and Table S1.

Experimental section

Chemicals and Materials: Vanadium chloride (VCl_3, Macklin, 99%), cobalt nitrate hexahydrate ($Co(NO_3)_2\cdot 6H_2O$, Aladdin, 99%), nitric acid (HNO_3, Aladdin, 65-68%), sulfuric acid (H_2SO_4, Aladdin, 98%), acetone (C_3H_6O, Sinopharm, 99%), ethanol (C_2H_6O, Tianjin DAMAO, 99%), urea (CH_4N_2O, Tianjin DAMAO, 99%), potassium hydroxide (KOH, Macklin, 95%), Pt/C (20 wt% Pt, Johnson Matthey), carbon cloth (W0S1009, Ce-Tech) were used as received. Deionized water (DI water for short) was used in all experiments.

Synthesis of V-doped cobalt hydroxide: A series of V-doped cobalt hydroxides were synthesized on carbon cloth through one-pot hydrothermal process. Firstly, a piece of carbon cloth substrate (CC for short, 3 cm × 3 cm) was sonicated for 15 min and soaked overnight in mixed acid, where the volume ratio of sulfuric acid (10 wt%) to nitric acid (10 wt%) is 1:3. Afterwards, the soaked CC was further treated with sonication in acetone, ethanol, and DI water for 10 min, respectively.

Typically, a certain amount of vanadium chloride, 0.69 g cobalt nitrate hexahydrate and 0.3 g urea were dissolved in 35 mL DI water. The received solution was transferred to 50 mL Teflon-lined stainless-steel autoclave, and pre-treated CC substrate was immersed in solution. Then the above system was sealed and heated at 120 °C for 12 h. After reaction, the system was cooled naturally, and the resulting CC was washed with DI water and ethanol and dried overnight at 60 °C to obtain V-doped cobalt hydroxide on CC, which was labeled as xV-$Co(OH)_2$/CC (x refers to the feed molar ratio of Co to V, and varies from 3 to 1). Additionally, the pure cobalt hydroxide on CC ($Co(OH)_2$/CC for short) was also prepared by the same process without adding vanadium source.

Characterization: The phase composition of as-prepared samples were recorded on X-ray diffractometer (XRD, Bruker D8 Advance) with Cu Kα radiation (λ = 0.154 nm). The surface morphologies and microstructures of materials were acquired through scanning electron microscopy (SEM, JSM-6701F) and transmission electron microscopy (TEM, FEI Tecnai G2 F30) equipped with energy dispersive spectrometer (EDS). The chemical composition and states of samples were analyzed using X-ray photoelectron spectroscopy (XPS, ESCALAB Xi+) with monochromatic Al Kα X-ray.

Electrochemical measurements: The electrochemical properties towards HER were evaluated by the three-electrode electrochemical system (CHI 760E, Chenhua Instruments, Shanghai) under alkaline condition (1 M KOH as electrolyte). Wherein the as-prepared xV-$Co(OH)_2$/CC (x=1, 2, and 3), $Co(OH)_2$/CC and bare CC were used as the working electrodes with 1 cm^2 area (1 cm × 1 cm), meanwhile, the graphite rod and Hg/HgO were employed as the counter and reference electrodes, respectively. Before electrocatalytic evaluation, the cyclic voltammetry (CV) was measured for 50 cycles at scan rate of 100 mV/s to ensure the stable contact between electrode and electrolyte. Afterwards, the linear sweep voltammetry (LSV) curves were measured at a scan rate of 5 mV/s, and the Tafer slope was further analyzed based on LSV data. The electrochemical impedance spectroscopy (EIS) was operated under a frequency from 0.01 Hz to 100 kHz with 5 mV AC amplitude. To compare the electrochemical double-layer capacitance (C_{dl}), the CV measurements were carried out at the potential of 0.02-0.12 V vs. RHE with different scan rates (10, 20, 30, 40, 50 mV/s). For the stability study of HER, the amperometric I-t curves were acquired at the current densities of 10 and 50 mA/cm^2 for 60 h. Here all the potentials without iR-correction were referenced to that of the reversible hydrogen electrode (RHE) by Nernst equation: $E_{RHE} = E_{Hg/HgO} + 0.0591 \times pH + 0.098$. In addition, the commercial Pt/C was also deposited on CC as working electrode for comparison.

Turnover frequency (TOF) calculation[1,2]: The TOF values of as-prepared catalysts were calculated according to the following equation:

$$\mathrm{TOF} = \frac{I}{2nF} \qquad (1)$$

where I represents the measured current (A) during LSV test, F is the Faraday constant (96485 C/mol) and n is the mole amount of active sites. The factor 1/2 accounts for two electrons consumed to form one H_2 molecule.

The value of n could be calculated by testing CV ranging from -0.2 to +0.6 V vs RHE in phosphate buffer solution (PBS, pH = 7) at a scan rate of 50 mV/s. The following formula was used to calculate the quantity of active sites (n):

$$n = \frac{Q}{2F} = \frac{i \cdot t}{2F} = \frac{i \cdot V/u}{2F} \qquad (2)$$

where Q is the cyclic voltammetric capacity obtained by integrating CV cures, F is the Faraday constant (96485 C/mol), i is the current (A), V is the voltage (V) and u is the scanning rate (V/s). The calculated n values for $Co(OH)_2$, 3V-$Co(OH)_2$, 2V-$Co(OH)_2$ and 1V-$Co(OH)_2$ were about 1.29×10^{-8}, 3.93×10^{-8}, 2.00×10^{-8} and 7.15×10^{-7} mol, respectively.

Computational section

All the calculations in this work were implemented using density-functional theory (DFT) in the Vienna ab initio Simulation Package (VASP) code.[3,4] The projector augmented wave (PAW) pseudopotentials can be used to describe the interaction between ionic cores and valence electrons.[5] The generalized gradient approximation (GGA) with Perdew-Burke-Ernzerh (PBE) functional was applied to deal with exchange correlation functions.[6,7] The DFT-D3 was considered to correct the interaction of van der Waals forces in all computation.[8] The cutoff energy of the plane-wave basis was set as 520 eV, and the convergence criteria for energy and force on each atom during geometry optimization were set to 10^{-4} eV and 0.01 eV/Å, respectively. The Brillouin zones were sampled with a k-point grid of 4×4×1 for all geometry optimization and electronic properties calculation.

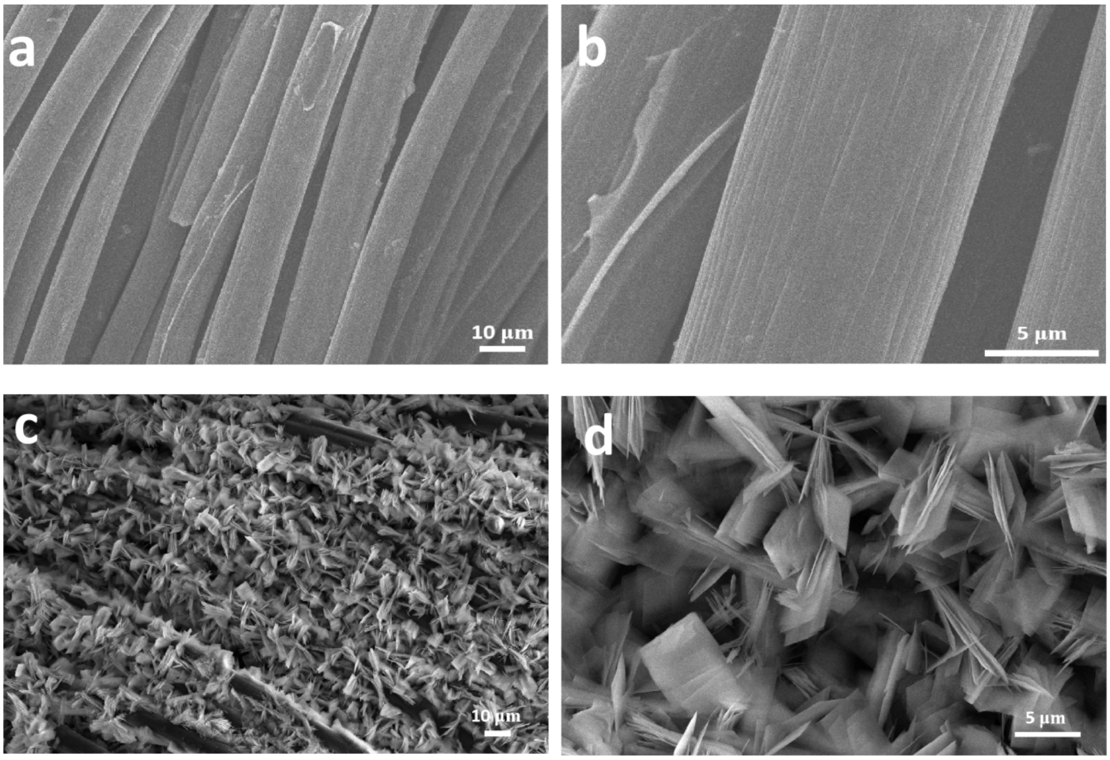

Fig. S1 SEM images of bare CC substrate (a, b), and pure $Co(OH)_2$ on CC (c,d).

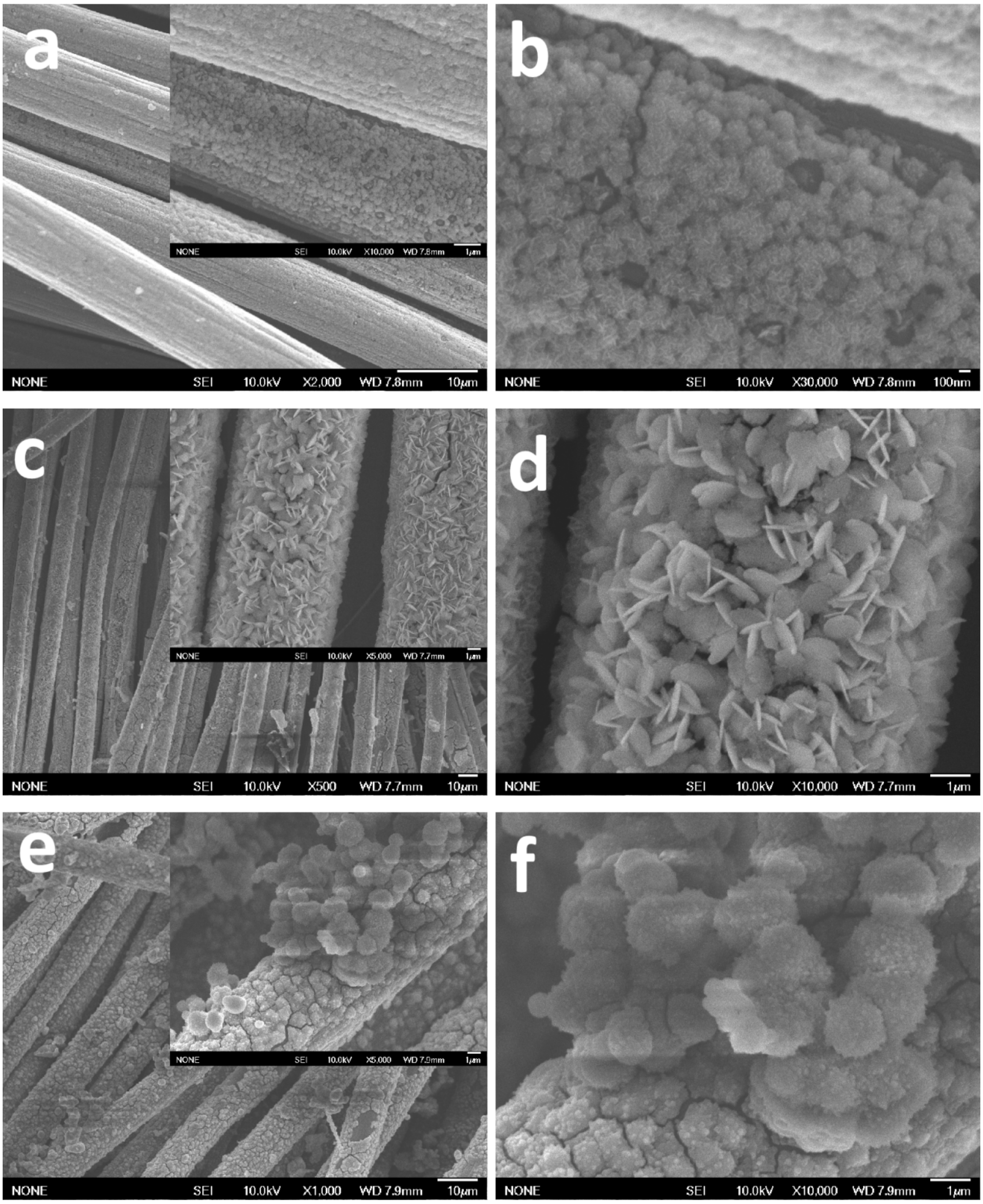

Fig. S2 SEM images of V-doped $Co(OH)_2$ on CC, including 3V-$Co(OH)_2$/CC (a, b), 2V-$Co(OH)_2$/CC (c, d), and 1V-$Co(OH)_2$/CC (e, f).

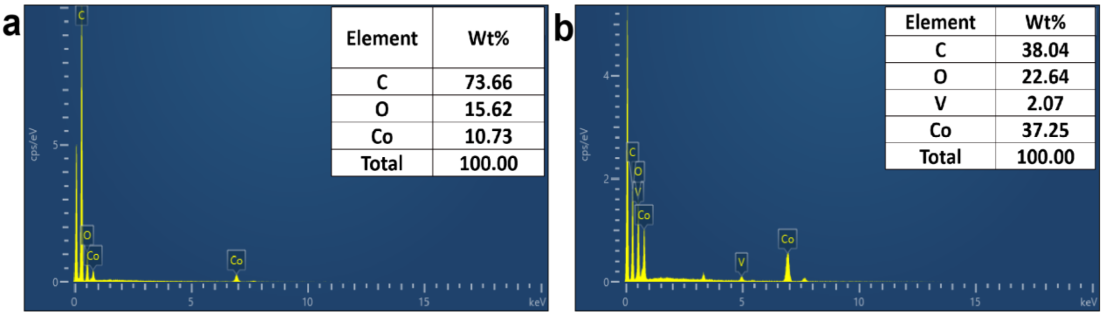

Element	Wt%
C	73.66
O	15.62
Co	10.73
Total	100.00

Element	Wt%
C	38.04
O	22.64
V	2.07
Co	37.25
Total	100.00

Fig. S3 EDS results of $Co(OH)_2$/CC (a) and V-$Co(OH)_2$/CC (b).

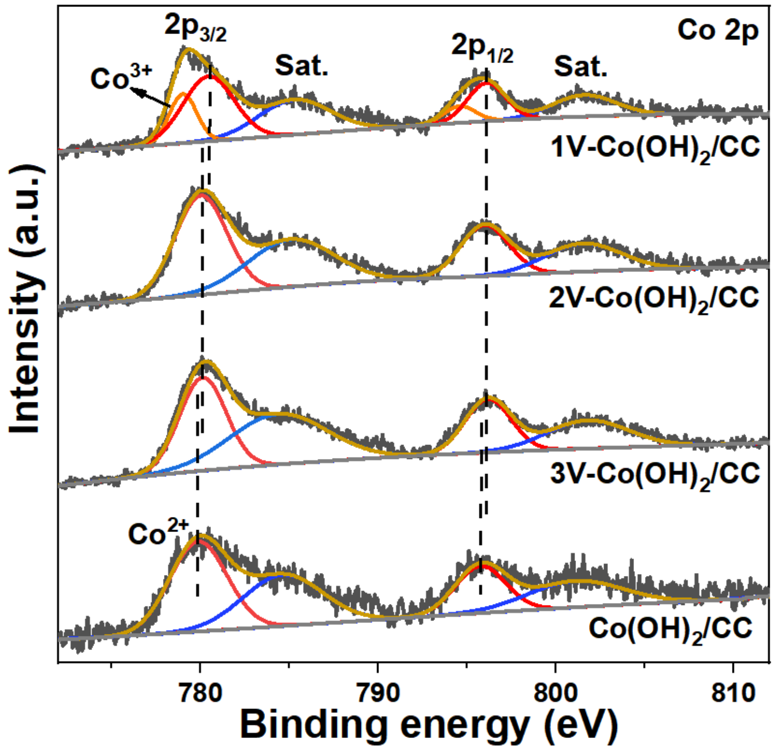

Fig. S4 Co 2p XPS spectra of $Co(OH)_2$/CC and V-$Co(OH)_2$/CC.

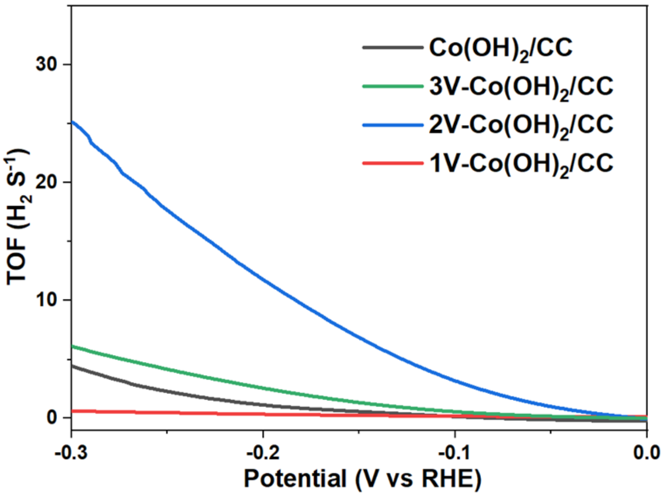

Fig. S5 TOF curves of Co(OH)$_2$/CC and V-Co(OH)$_2$/CC.

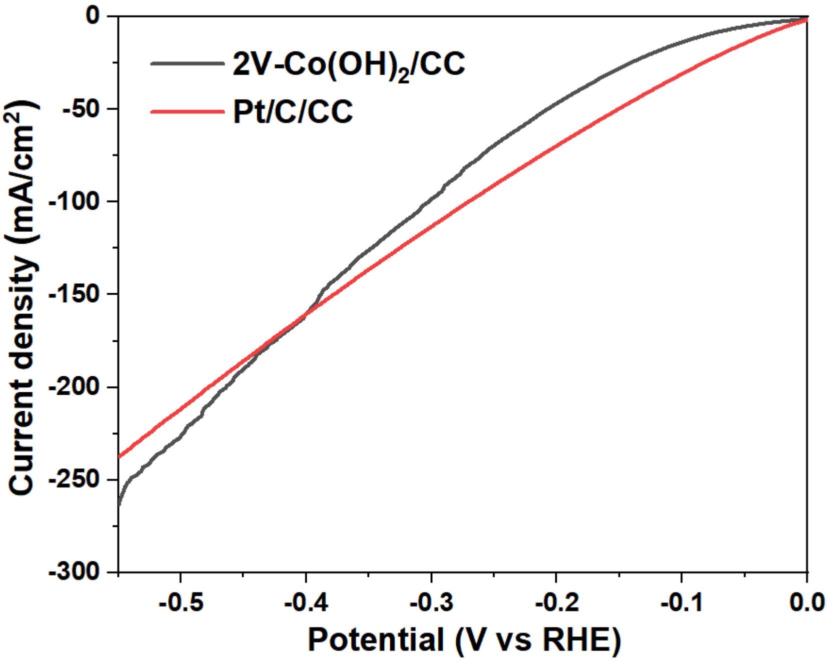

Fig. S6 HER polarization curves of 2V-$Co(OH)_2$/CC and commercial Pt/C deposited on CC.

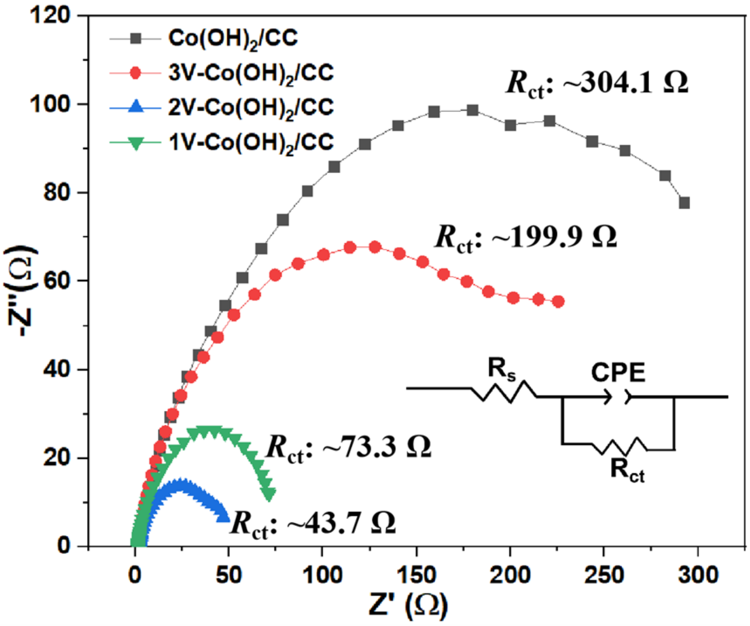

Fig. S7 Nyquist plots of $Co(OH)_2$/CC and V-$Co(OH)_2$/CC. The inset shows the corresponding equivalent circuit, where R_s is attributed to the solution resistance, constant-phase element (CPE) refers to the double layer capacitance, and R_{ct} represents the charge-transfer resistance.

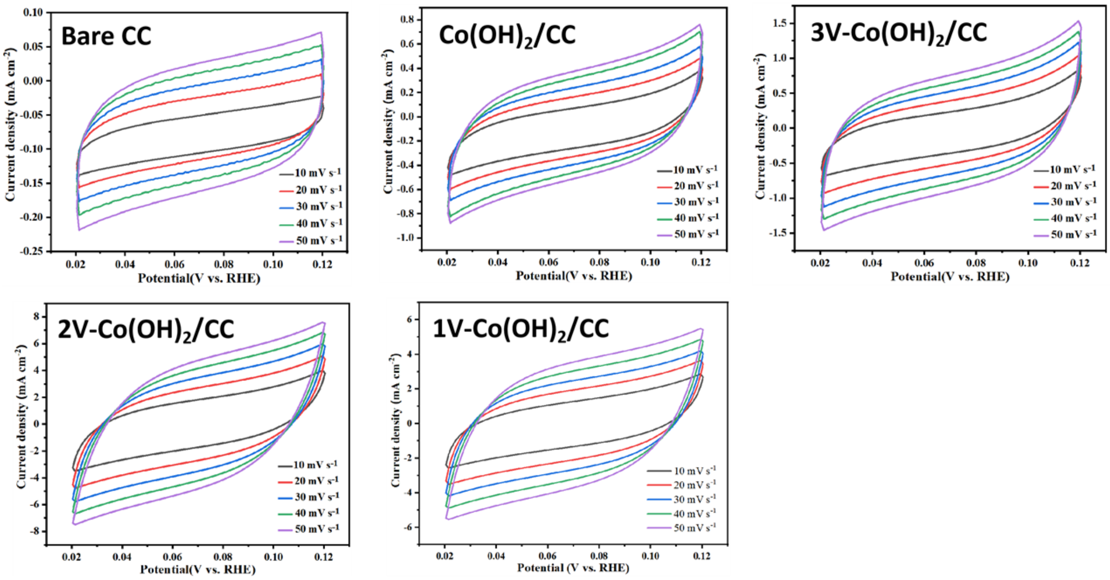

Fig. S8 Cyclic voltammetry curves of the samples at the potential of 0.02-0.12 V vs. RHE with different scan rates (10, 20, 30, 40, 50 mV/s).

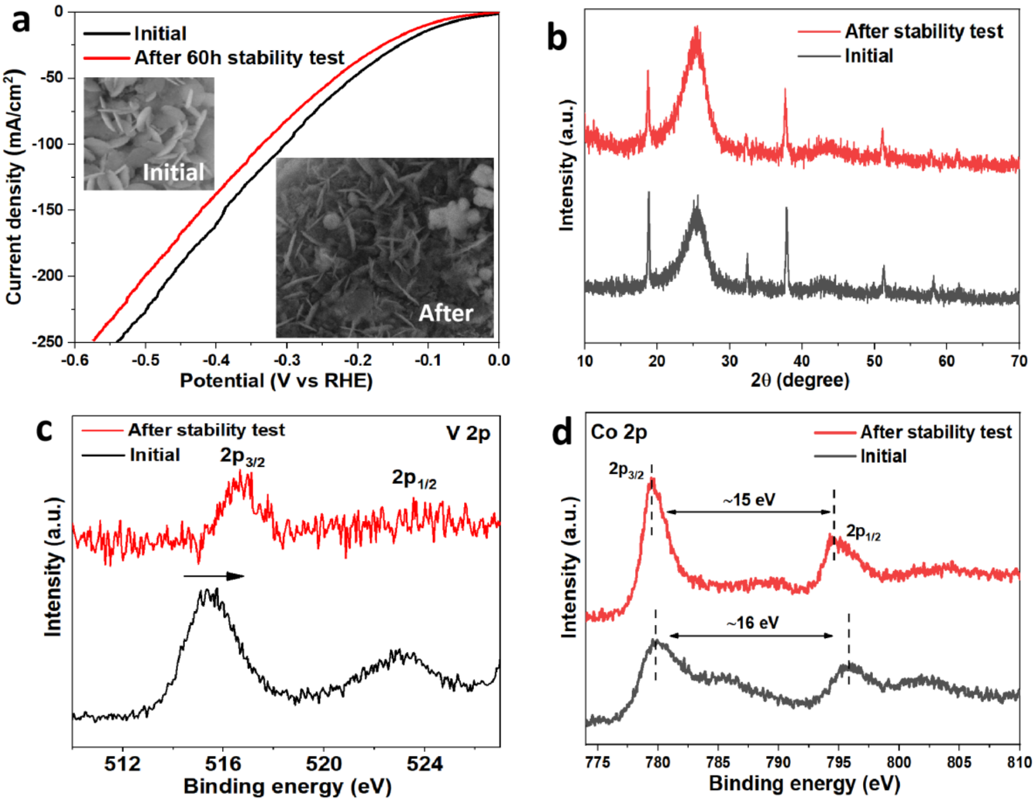

Fig. S9 HER polarization curves of 2V-Co(OH)$_2$/CC before and after 60 h stability test (a) and the corresponding XRD patterns (b) and XPS spectra (c, d). The inset of Fig. S6a is the SEM images of 2V-Co(OH)$_2$/CC before and after test.

The SEM images (inset of Fig. S9a) show the regular nanosheets partially suffer collapse and agglomeration after stability test, which may be the cause of the reduced catalytic activity. Afterwards, the XRD and XPS were also carried out to study the phase composition and surface chemical states of 2V-Co(OH)$_2$/CC after stability test. As indicated in Fig. S9b, the XRD pattern coincides with the initial one, demonstrating the phase composition of 2V-Co(OH)$_2$/CC remains unchanged. For XPS results, the decreased XPS signals and shifted XPS peaks are observed in V 2p spectrum after stability test (Fig. S9c), implying the dissolution of doped V element and the slight change of surface chemical states. Meanwhile, in Co 2p spectra (Fig. S9d), the spin energy separation between Co 2p$_{1/2}$ and Co 2p$_{3/2}$ is reduced to ~15 eV, which indicates the coexist of Co^{2+} and Co^{3+}.[9] The combined characterization results show the intrinsic phase composition of 2V-$Co(OH)_2$/CC is retained, while the surface morphology and electronic structures are changed after a long-term HER test, thus, the 2V-$Co(OH)_2$/CC displays a slight decrease in HER activity.

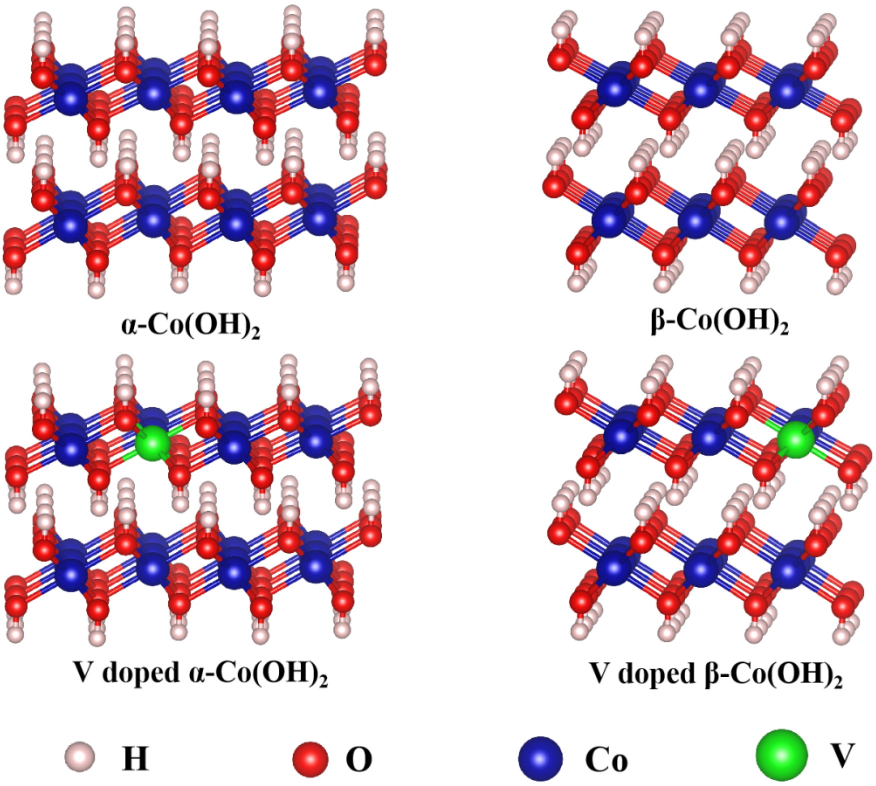

α-$Co(OH)_2$

β-$Co(OH)_2$

V doped α-$Co(OH)_2$

V doped β-$Co(OH)_2$

Fig. S10 Geometric configurations of α-$Co(OH)_2$, β-$Co(OH)_2$ and V-doped $Co(OH)_2$.

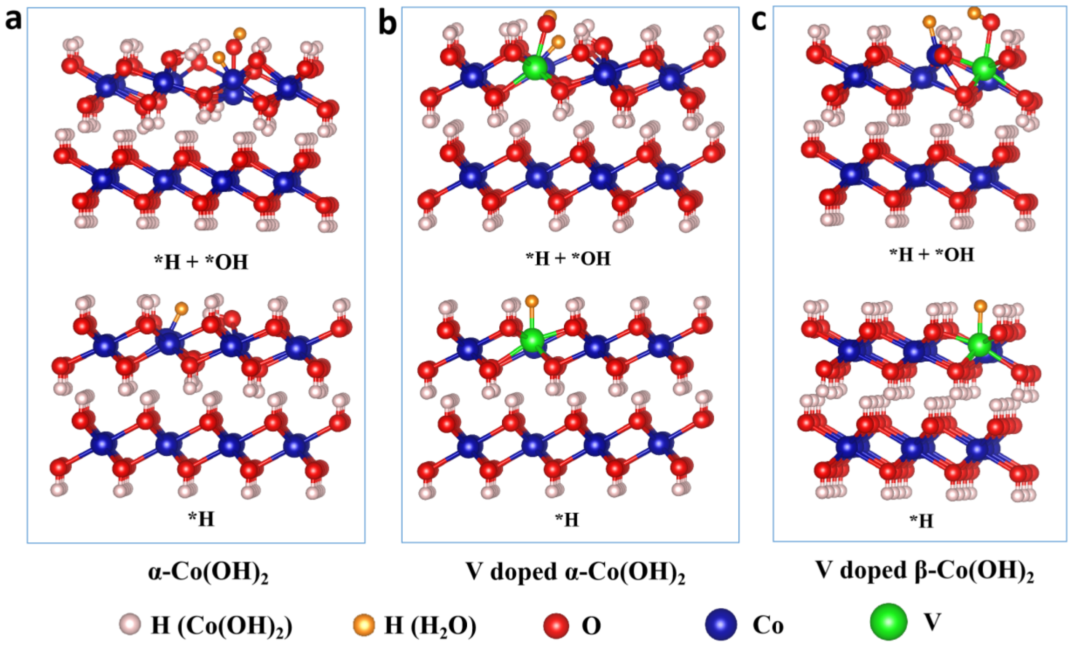

Fig. S11 Transition states of water dissociation on α-$Co(OH)_2$ (a), V-doped α-$Co(OH)_2$ (b), and V-doped β-$Co(OH)_2$ (c).

Table S1. The comparison of HER performance of recently reported cobalt-/hydroxide-based catalysts in alkaline media

Catalyst	**Substrate**	**Electrolyte**	**η_{10} (mV vs RHE)**	**η_{100} (mV vs RHE)**	**Tafel slope (mV/dec)**	**Reference**
V-$Co(OH)_2$	Carbon cloth	1M KOH	83	303	111.7	This work
NiFe-LDH/$Ni(OH)_2$	Ni foam	1 M KOH	155	270	112	10
O_V-NiFe-LDH	Ni foam	0.1 M KOH	161	N/A	126	11
Pd-$CoSe_2$	Glass carbon	1 M KOH	240	N/A	92	12
Mo-$Co_{0.85}Se$/NC	N/A	1 M KOH	151	234	51	13
Fe-CoP/$Ni(OH)_2$	Ni foam	1 M KOH	91	N/A	48	14
$Co(OH)_x$@CoP	Glassy carbon	1 M KOH	100	250	76	15
N-c-$CoSe_2$	Carbon fiber cloth	1 M KOH	98	224	63.4	16
Mn-O@Co-P	Carbon cloth	1 M KOH	106	170	56	17
B-doped CoP/Ni_2P	Glassy carbon	1 M KOH	78	N/A	73	18
Re-NiFeOH	Carbon cloth	1 M KOH	~92	243	46	19

Notes and references

1 Y. Shi, Z.-R. Ma, Y.-Y. Xiao, Y.-C. Yin, W.-M. Huang, Z.-C. Huang, Y.-Z. Zheng, F.-Y. Mu, R. Huang, G.-Y. Shi, Y.-Y. Sun, X.-H. Xia and W. Chen, *Nat. Commun.*, 2021, **12**, 3021.

2 L. Zeng, K. Sun, X. Wang, Y. Liu, Y. Pan, Z. Liu, D. Cao, Y. Song, S. Liu and C. Liu, *Nano Energy,* 2018, **51**, 26-36.

3 G. Kresse and J. Hafner, *Phys. Rev., B Condens.*, 1993, **47**, 558-561.

4 G. Kresse, J. Furthmiiller. *Comput. Mater. Sci.*, 1996, **6**, 15-50.

5 P. E. Blochl, *Phys. Rev., B Condens.*, 1994, **50**, 17953-17979.

6 G. Kresse and D. Joubert, *Phys. Rev., B Condens.*, 1999, **59**, 1758-1775.

7 J. P. Perdew, K. Burke and M. Ernzerhof, *Phys. Rev. Lett.*, 1996, **77**, 3865-3868.

8 S. Grimme, J. Antony, S. Ehrlich and H. Krieg, *J. Chem. Phys.*, 2010, **132**, 154104.

9 K. Xiang, D. Wu, X. Deng, M. Li, S. Chen, P. Hao, X. Guo, J.-L. Luo and X.-Z. Fu, *Adv. Funct. Mater.*, 2020, **30**, 1909610.

10 N. S. Gultom, H. Abdullah, C.-N. Hsu and D.-H. Kuo, *Chem. Eng. J.*, 2021, **419**, 129608.

11 W. H. Lee, M. H. Han, U. Lee, K. H. Chae, H. Kim, Y. J. Hwang, B. K. Min, C. H. Choi and H.-S. Oh, *ACS Sustainable Chem. Eng.*, 2020, **8**, 14071-14081.

12 X. Zhao, X. Li, D. Xiao, M. Gong, L. An, P. Gao, J. Yang and D. Wang, *Appl. Catal. B-Environ.*, 2021, **295**, 120280.

13 Q. Dai, L. Wang, K. Wang, X. Sang, Z. Li, B. Yang, J. Chen, L. Lei, L. Dai and Y. Hou, *Adv. Funct. Mater.*, 2022, **32**, 2109556.

14 X. Yu, J. Zhao and M. Johnsson, *Adv. Funct. Mater.*, 2021, **31**, 2101578.

15 L. Su, X. Cui, T. He, L. Zeng, H. Tian, Y. Song, K. Qi and B. Y. Xia, *Chem. Sci.*, 2019, **10**, 2019-2024.

16 Y. Sun, X. Li, T. Zhang, K. Xu, Y. Yang, G. Chen, C. Li and Y. Xie, *Angew. Chem.*, 2021, **133**, 21745-21752.

17 D. Zhou, Z. Wang, X. Long, Y. An, H. Lin, Z. Xing, M. Ma and S. Yang, *J. Mater.*

Chem. A, 2019, **7**, 22530-22538.

18 M. Liu, Q. He, S. Huang, W. Zou, J. Cong, X. Xiao, P. Li, J. Cai and L. Hou, *ACS Appl. Mater. Interfaces*, 2021, **13**, 9932-9941.

19 S. B. Roy, E. Jung, K. H. Kim, A. Patil, S.-H. Chun, J. H. Park and S. C. Jun, *Chem. Eng. J.*, 2022, **435**, 135184.